의학과 석사 학위논문

Combined Fluid-attenuated Inversion Recovery and Fat Suppression MR Imaging for Cartilage Evaluation: An Ex Vivo Study Using Porcine Patella

연골 평가를 위한 지방-물 이중 억제 자기공명영상: 돼지 슬개골을 이용한 생체 외 연구

2020년 7월

서울대학교 대학원

의학과 영상의학전공

박성은

의학과 석사 학위논문

Combined Fluid-attenuated Inversion Recovery and Fat Suppression MR Imaging for Cartilage Evaluation: An Ex Vivo Study Using Porcine Patella

연골 평가를 위한 지방-물 이중 억제 자기공명영상: 돼지 슬개골을 이용한 생체 외 연구

2020년 7월

서울대학교 대학원

의학과 영상의학전공

박성은

연골 평가를 위한 지방-물 이중 억제 자기공명영상: 돼지 슬개골을 이용한 생체 외 연구

지도교수 홍성환

이 논문을 의학 석사 학위논문으로 제출함

2020년 05월

서울대학교 대학원

의학과 영상의학전공

박성은

박성은의 의학석사 학위논문을 인준함

2020년 7월

위 원 장 천 정 은 (인)

부위원장 홍 성 환 (인)

위 원 장 종 범 (인)

Abstract

Combined Fluid-attenuated Inversion Recovery and Fat Suppression MR Imaging for Cartilage Evaluation: An Ex Vivo Study Using Porcine Patella

Sungeun Park
Department of Radiology, College of Medicine
The Graduate School
Seoul National University

Objectives

To describe the imaging characteristics of combined fluid-attenuated inversion recovery with fat suppression (FLAIR-FS) in cartilage imaging and compare its basic features with those of conventional MR sequences.

Methods

MR images of 14 porcine patellae were obtained with a 3-T MR imaging unit. A normal-saline-filled plastic container, containing two porcine patellae fixed with rubber bands, was positioned in the coil. The MR imaging sequences included T1-weighted

imaging (T1WI), T2-weighted imaging (T2WI), and FLAIR-FS with an inversion time of 1500 ms. In the last two of the 14 patellae, the double-echo steady-state (DESS) (TR/TE = 14.5/5.0, flip angle 30°, slice thickness 1.0 mm) and ultrasonography (US) were additionally performed. For 28 annotated points on 14 patellae, visual grading of cartilage layer conspicuity was performed with 5-point scores on T1-, T2WI, and FLAIR-FS by two MSK radiologists. As a hypointense layer at the cartilage-water interface was unexpectedly seen with FLAIR-FS, we examined whether the interfacial hypointense layer was a part of the cartilage by comparing between FLAIR-FS and DESS. In the last two patellae with additional DESS and US scans, composite images from FLAIR-FS and DESS were made to inspect the location of the interfacial hypointense layer with FLAIR-FS relative to DESS. We also compared cartilage thickness measurements between FLAIR-FS and DESS. For FLAIR-FS, two different methods of cartilage thickness measurement were applied, including or excluding the interfacial hypointense layer. To verify the accuracy of cartilage thickness measurements on DESS, the measurements on MRI and US were compared. The degree of absolute agreement between measurements was obtained using the intraclass correlation coefficient (ICC) with a 95% confidence interval.

Results

FLAIR-FS (TI 1500 ms) resulted in moderate water signal suppression and showed a higher signal intensity for the articular cartilage than free water. T1WI, T2WI, and FLAIR-FS showed a trilaminar appearance of the articular cartilage. This layered appearance was most pronounced with FLAIR-FS, followed by T2WI and T1WI ($p < 0.001$). A thin hypointense layer (0.7 ± 0.1 mm in thickness) appeared at the cartilage-water interface with FLAIR-FS. By excluding the interfacial hypointense layer, the cartilage

surfaces matched well each other on composite image of FLAIR-FS and DESS. The cartilage thickness of the DESS reference standard was 2.2 ± 0.4 mm. When we compared cartilage thickness measurements on DESS and FLAIR-FS, exclusion of the interfacial hypointense layer (2.3 ± 0.3 mm, absolute ICC agreement 0.904) produced greater agreement than inclusion (3.0 ± 0.2 mm, absolute ICC agreement 0.322). The ICC of absolute agreement was 0.919 in comparison between DESS and US cartilage thickness measurements.

Conclusions

FLAIR-FS showed superior contrast between cartilage layers and revealed a potential restricted water layer at the cartilage-water interface.

Keywords

Cartilage, Magnetic resonance image, Fluid-attenuated inversion recovery, Fat suppression

Student Number: 2018-26078

Contents

List of Tables and Figures

Figure 4. (a) Composite image of DESS and FLAIR-FS with landmark holes (arrows). The left half is from DESS, and the right half is from FLAIR-FS. The cartilage surface with DESS correlates with that with FLAIR-FS by excluding the interfacial hypointense layer at the cartilage-water interface. Note that the landmark hole with FLAIR-FS is also 'covered' by the interfacial hypointense layer. (b) Corresponding ultrasound image with landmark holes (arrows).

Introduction

Magnetic resonance (MR) imaging is the most important imaging modality for the evaluation of traumatic or degenerative cartilaginous lesions in the knee (1). Many MR imaging techniques are available to facilitate the assessment of cartilage morphology in the knee, two-dimensional fast spin echo sequences with intermediate-weighted and T2-weighted contrast are the most common sequences used in clinical practice to evaluate articular cartilage (2, 3). An effective T2 weighting for visualization of cartilage should produce images that distinguish cartilage from synovial fluid and allow for visualization of the internal structure of cartilage as revealed in the presence of layers (4, 5).

Human articular cartilage can be divided histologically into four zones: superficial or tangential, transitional, radial and calcified zones. On MR imaging, normal cartilage has a bilaminar or trilaminar appearance depending on the pulse sequence used. Layers or laminae of varying signal intensity are the characteristic feature of MR images of normal articular cartilage. The layers reflect the presence of depth-dependent variations in the T2 of cartilage, and the boundaries between layers are not discrete or well defined due to gradual variation in T2. Fast spin echo T2-weighted imaging provides excellent contrast between the synovial fluid and cartilage surface, however it suffers from a relatively low contrast between cartilage layers due to limited dynamic range. Fat suppression is a good remedy for poor intrinsic cartilaginous contrast of T2-weighted imaging. Suppression of the signal from fat in the subcutaneous tissues or subchondral bone improves the dynamic range and eliminates chemical shift artifacts for cartilage imaging (6).

In a recent study (7) assessing peripatellar synovitis with combined fluid-attenuated inversion recovery and fat suppression MR imaging (FLAIR-FS) on 3-T MRI, we incidentally observed a pronounced contrast between cartilage layers of bilaminar

appearance. In our practice, FLAIR-FS seemed more clearly to distinguish a high signal superficial layer and a lower signal intensity deep layer of the patellar cartilage than conventional fluid-sensitive sequences in the knee MRI. These imaging characteristics may help to more sensitively detect not only cartilage defects but also early-stage cartilage signal abnormalities. Cartilage signal abnormalities represent early abnormal changes in the cartilage, which eventually may develop into morphologic defects (8).

Fat suppression techniques have been widely used to improve the tissue contrast of musculoskeletal structures including articular cartilage. To our knowledge, however, water suppression techniques have never been applied to cartilage imaging. On FLAIR-FS, the water signal can be controlled and adjusted, and water suppression may result in new contrast between cartilage layers and at the cartilage-water interface. In this regard, FLAIR-FS could be a new candidate for morphologic imaging of articular cartilage and a potential tool to explore interfacial phenomena on the surface of hydrated cartilage.

Our study aimed to describe the imaging characteristics of FLAIR-FS in cartilage imaging and to compare its basic features with those of conventional MR sequences, using porcine patella.

Materials and Methods

Sample preparation

This study was exempt from the requirements of the institutional animal care and use committee. Freshly excised 5- to 6-month-old porcine patellae were obtained from a local slaughterhouse. Surrounding soft tissue was carefully removed from the patellae. Visual inspection of the patellae was performed to detect morphologic defects or cracks in the cartilage, and 14 patellae without gross abnormalities were selected for imaging studies.

Image acquisition

The MR images were obtained with a 3-T MR imaging unit (TrioTim; Siemens, Erlangen, Germany) with an eight-channel knee coil (Invivo, Florida, U.S.A.), with an inner diameter of 13 cm. The coil was placed at the isocenter of the MR unit. A plastic container filled with normal saline, containing two porcine patellae fixed with rubber bands, was positioned in the coil, and so two patellae were imaged at a time.

The MR imaging sequences included fast spin echo T1-weighted (T1WI; TR/TE = 650.0/9.8), T2-weighted (T2WI; TR/TE = 3000.0/99.0), and FLAIR-FS (TR/TE = 9000.0/85.0, TI = 1500 ms) sequences. For FLAIR-FS, a 180° inversion pulse and a 90° excitation radiofrequency pulse were applied, and then a saturation pulse was applied for chemical shift–selective fat suppression. We determined the inversion time to be 1500 ms for moderate water signal suppression after having tried different numbers of inversion times (TI = 1300, 1500, 1700, 1900, 2100, 2300 ms). The imaging parameters were as follows: matrix size 384 × 269; number of excitations 4.0; field of view 14 × 14 cm and slice thickness 2.5 mm.

In the last two of the 14 patellae, the double-echo steady-state (DESS) (TR/TE = 14.5/5.0, flip angle 30°, slice thickness 1.0 mm) and ultrasonography (US) were additionally performed. To match imaging planes between MR imaging and US, artificial holes were made with a 15-gauge biopsy drill (Bonopty bone biopsy system, Radi Medical Systems, Uppsala, Sweden) (Fig. 1).

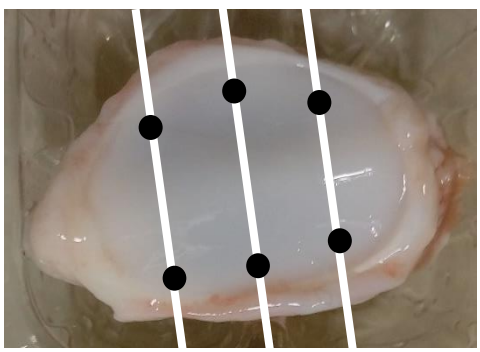

Figure 1. Black points represent artificial holes drilled on each side of the patella (three holes on each side and a total of six holes on one patella), which define three imaginary parallel lines (white lines)

The cartilage US (Epiq 5, Philips, Bothel, WA, USA) was performed with an 18 MHz linear probe on the same day of MR imaging.

Visualization of cartilage layers with FLAIR-FS

A total of fourteen patellae were used to evaluate the contrast between layers of the articular cartilage. One radiologist (S.E.P., 4 years of experience in musculoskeletal imaging) selected an axial image of each patella where the cartilage surface was imaged most perpendicularly. Then, two points, 7 mm apart from each end of a patella, were annotated on the chosen images (a total of 28 points) (Fig. 2). For the annotated points of

each patella, visual grading of cartilage layer conspicuity was performed with 5-point scores (4: excellent, 3: good, 2: fair, 1: subtle, 0: none) on three sequences (T1WI, T2WI and FLAIR-FS) by two MSK radiologists (S.H.H. and H.J.Y., with 26 and 5 years of experience in musculoskeletal imaging, respectively). The two reviewers were provided with illustrations and MRI examples from the pilot study (Fig. 2). All images were viewed on a picture archiving and communication system workstation (Gx; Infinit Technology, Seoul, Korea).

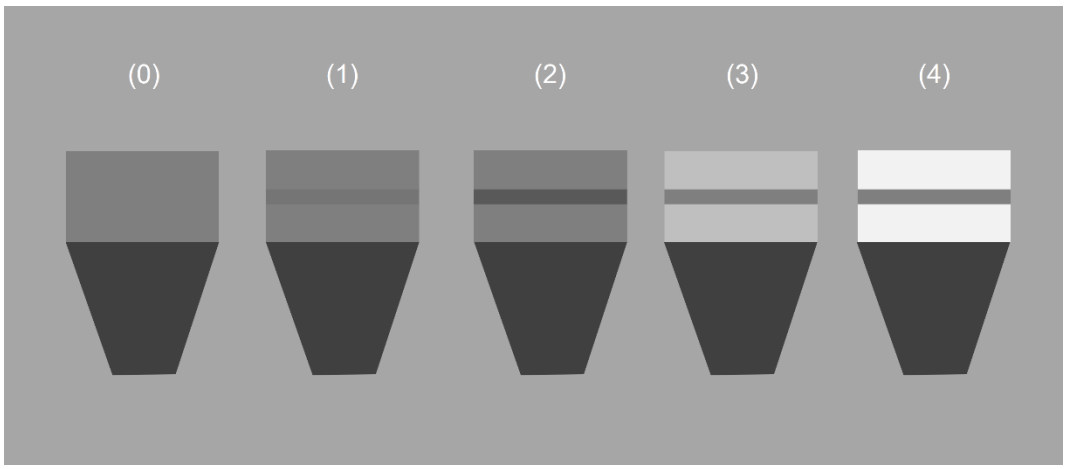

Figure 2. Illustration of cartilage layer 5-point score grading

(0): None. No detectable layered pattern.

(1): Subtle. Barely detectable layered appearance.

(2): Fair. Visible layered appearance, with narrow dynamic range.

(3): Good. Definite layered appearance, with moderate dynamic range.

(4): Excellent. Definite layered appearance, with wide dynamic range.

Analysis of the cartilage-water interface with FLAIR-FS

As a hypointense layer at the cartilage-water interface was unexpectedly seen with

FLAIR-FS, we attempted to determine whether this interfacial hypointense layer was a part of the cartilage. In the last two patellae with additional DESS and US scans, composite images from FLAIR-FS and DESS were made to inspect the location of the interfacial hypointense layer with FLAIR-FS relative to DESS (Fig. 3a). We also compared cartilage thickness measurements between FLAIR-FS and DESS. For FLAIR-FS, two different methods of cartilage thickness measurement were applied, including or excluding the interfacial hypointense layer. Those measurements with FLAIR-FS were compared with measurements with DESS, which were used as reference standards of cartilage thickness. To verify the accuracy of DESS for cartilage thickness measurement, a supplementary comparison of cartilage thickness measurements between DESS and US was made (Fig. 3b). At ultrasound, cartilage thickness was measured perpendicular to the cartilage surface and between the leading edges of the two echo zones at cartilage surface and cartilage-bone interface (9, 10). The cartilage thickness measurements on MR images and US were performed on four out of six imaginary lines in the two patellae, which matched well between MR images and US. All measurements were performed by one radiologist (S.E.P.) at 20 points: 3 and 5 mm apart from the landmark holes and center (ridge) of the imaginary lines.

Terminology for the layered structures

In this study, the terms ‘layer’ or ‘lamina’ was reserved for the description of the layered structure inside and around the cartilage on MRI. The term ‘zone’ refers to the histological zone in the cartilage.

Statistical analysis

The visual grading scores assigned by two reviewers were averaged, considering the subjective nature of the scoring system. Then, Wilcoxon's signed rank test was used to compare the average scores of cartilage layer conspicuity between different imaging sequences. For cartilage thickness measurements, the degree of absolute agreement between measurements was obtained using the intraclass correlation coefficient (ICC) with a 95% confidence interval. The SPSS statistical package (version 25.0 for Windows, SPSS) was used for statistical analysis. P values less than 0.05 were considered to indicate statistical significance.

Sample size estimation

Sample size estimation was conducted using the software G*Power 3.1.9.2 (Franz Faul, Kiel University, Germany), with 80% power and a one-tailed alpha error of 0.05 (11, 12). From our pilot study for visual grading of cartilage layer conspicuity, the anticipated effect size was 0.8 and the calculated sample size was 12. Finally, a total of 14 patellae were prepared with a potential drop-out of two.

Results

Visualization of cartilage layers with FLAIR-FS

FLAIR-FS with 1500 ms TI resulted in moderate water signal suppression and showed higher signal intensity of the articular cartilage than free water (Fig. 2). There was a thin hypointense layer at the cartilage-water interface with FLAIR-FS, and it was first unclear whether this layer was a part of the articular cartilage. Except for the interfacial hypointense layer, FLAIR-FS showed a trilaminar structure, which comprised high-low-high signal layers from the superficial to the deep portion of the cartilage.

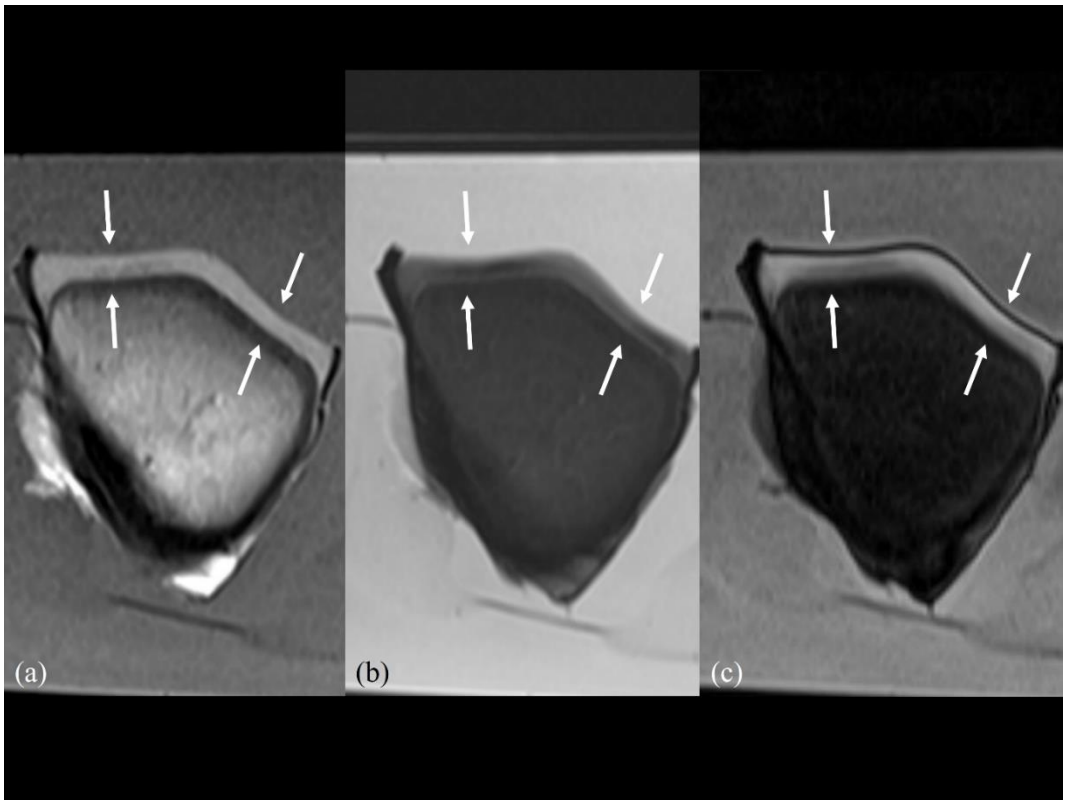

Figure 3. Cartilage layer conspicuity. (a) A T1-weighted image showing a trilaminar appearance with a faint low signal middle layer. Two points were given score 1 by two

reviewers. (b). A T2-weighted image showing a trilaminar appearance with a relatively hypointense middle layer. Two points given score 2 by two reviewers. (c). A FLAIR-FS image showing a trilaminar appearance (except the hypointense layer at the cartilage-water interface) consisting of high-low-high signal layers from the superficial to the deep portion. Left point was given score 4 and right point was given score 3 by two reviewers.

T1- and T2WIs also showed a trilaminar appearance of the articular cartilage, consisting of high-low-high signal layers from the superficial to the deep portion. At the cartilage-water interface, neither T1- nor T2WIs showed an interfacial hypointense layer, which was seen with FLAIR-FS. In some patellae, T1WI showed an almost homogeneous signal of the articular cartilage, and the middle hypointense layer was barely seen. Although T2WI showed a layered structure of the articular cartilage, all layers had markedly low signal when compared to that of water. Consequently, the laminar structure of the articular cartilage was most pronounced with FLAIR-FS, followed by T2WI and T1WI (Table 1).

Table 1. Grading of cartilage layer conspicuity.

Sequence	**Score**
T1WI	0.7 ± 0.6
T2WI	1.3 ± 0.7
FLAIR-FS	2.4 ± 1.0
P values of the Wilcoxon signed rank test	
T1WI, T2WI	0.001
T1WI, FLAIR-FS	< 0.001
T2WI, FLAIR-FS	< 0.001

Note - Score 4 = excellent, 3 = good, 2 = fair, 1 = subtle, 0 = none

Analysis of cartilage-water interface with FLAIR-FS

On composite MR images, parts of the patella from FLAIR-FS and DESS were well registered (Fig. 3a). When the interfacial hypointense layer was regarded as the cartilage surface, there was a step-off between the cartilage surfaces with FLAIR-FS and DESS. By excluding the interfacial hypointense layer, the cartilage surfaces matched well with each other between FLAIR-FS and DESS. Of note, the landmark hole with FLAIR-FS was also ‘covered’ or ‘coated’ by the interfacial hypointense layer.

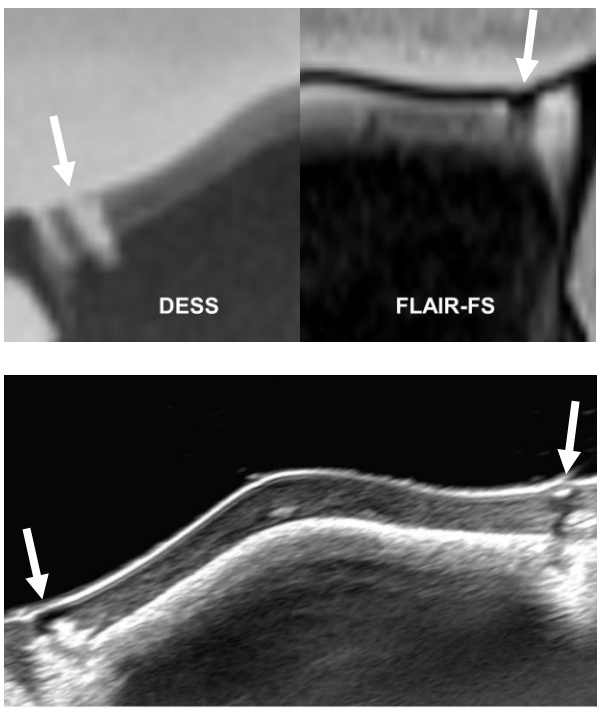

Figure 4. (a) Composite image of DESS and FLAIR-FS with landmark holes (arrows). The left half is from DESS, and the right half is from FLAIR-FS. The cartilage surface with DESS correlates with that with FLAIR-FS by excluding the interfacial hypointense layer at the cartilage-water interface. Note that the landmark hole with FLAIR-FS is also ‘covered’ by the interfacial hypointense layer. (b) Corresponding ultrasound image with landmark holes (arrows).

The cartilage thickness of the reference standard using DESS was 2.2 ± 0.4 mm. The thickness of the hypointense layer at the cartilage-water interface with FLAIR-FS was 0.7 ± 0.1 mm. When we compared cartilage thickness measurements with DESS and FLAIR-FS, cartilage thickness measurements excluding the interfacial hypointense layer (2.3 ± 0.3 mm, ICC of absolute agreement 0.904) showed higher agreement than those including the layer (3.0 ± 0.2 mm, ICC of absolute agreement 0.322). Comparing cartilage thickness measurements with DESS and US, the ICC of absolute agreement was 0.919 (Table 2).

Table 2. Cartilage thickness measurements

MR sequence/modality	**Thickness (mm)**	**ICC with DESS (95% CI)**
DESS	2.2 ± 0.4	(-)
FLAIR-FS excluding IHL	2.3 ± 0.3	0.904 (0.758 – 0.962)
FLAIR-FS including IHL	3.0 ± 0.2	0.322 (-0.065 – 0.728)
Ultrasound	2.1 ± 0.3	0.919 (0.674 – 0.973)

Note - FLAIR-FS: combined fluid-attenuated inversion recovery with fat suppression

DESS: double-echo steady-state

IHL: the interfacial hypointense layer at the cartilage-water interface.

Discussion

Our experimental study showed two notable features of FLAIR-FS in cartilage imaging. By moderately suppressing the free water signal, we observed a more prominent contrast between cartilage layers with FLAIR-FS than on conventional T1- or T2WIs. More curiously, FLAIR-FS showed a thin hypointense layer at the cartilage-water interface, which was most likely a restricted water layer in the vicinity of the cartilage surface. Hence, our results imply that FLAIR-FS is useful to demonstrate layered structures inside and outside hydrated articular cartilage in water.

Grunder (13) presented three laminae of the patellar cartilage of juvenile pigs consisting of middle hypointense lamina and higher signal superficial and deep laminae on T2WI. Our results showed similar trilaminar appearance on T1-, T2WI and FLAIR-FS, although the thickness of each lamina and contrast between laminae were not constant among the three sequences. It is clear that both intrinsic factors of tissue (T1 and T2 relaxation) and operating factors (TR, TE, TI) led to these differences. The T2 value is the major determinant of the tissue contrast of articular cartilage, and depth-dependent variability in T2 causes a characteristic laminar appearance in MRI images of cartilage. This regional variation in the signal intensity is largely due to variations in the orientation of the collagen fibrils relative to the magnetic field (14). On the other hand, T1WI showed a faint contrast between laminae. It has been known that T1 weighting has little effect on the overall laminar pattern due to the rather uniform T1 profile across the depths of the articular cartilage (15).

The T2-weighted imaging sequences showed excellent contrast differences due to the fluid-cartilage interface but at the expense of a reduced signal from the articular cartilage (16). Fat suppression techniques enhance the contrast between cartilage layers

because of the expanded dynamic range available with such techniques (4). In our study, we were able to further improve cartilage layer conspicuity by adding water suppression to fat suppression. FLAIR-FS with TI 1500 ms resulted in moderate suppression of the free water signal along with the elimination of fat signal and additional increase in dynamic range within the articular cartilage. FLAIR-FS showing such an increased contrast could be helpful for detecting pathologic changes of the articular cartilage at an early, perhaps reversible, stage.

Histologically, articular can be separated into 4 zones: superficial or tangential, transitional, radial and calcified zones. The superficial surface, which is composed of collagen fibers predominantly parallel to the surfaces, provides a low friction and bearing load in a high-speed situation. Taken together, the fluid film and boundary lubrication in the water-based lubricant environment lead to the low friction of articular cartilage (17). At the most superficial aspect of the articular surface, there is a thin layer called the lamina splendens (18). In a recent study, this uppermost superficial surface layer was found to provide a lubricating boundary, in which the main molecular constituents were hyaluronic acid, aggrecans, lubricin and phospholipids (19). Atomic force microscopy analysis revealed that the thickness of the uppermost superficial surface layer was 800 nm ~ 2 μm in porcine patellar articular cartilage (20).

In our experiment, we observed a thin hypointense layer at the cartilage-water interface with FLAIR-FS. Given that the thickness of the interfacial hypointense layer was 0.7 ± 0.1 mm, it could not be the lamina splendens of the articular cartilage. Through comparison of cartilage thickness measurements, it was also found that the interfacial hypointense layer was not a part of cartilage but a layer located just outside the cartilage. We used DESS as an internal standard for cartilage thickness because it has been used in

various knee osteoarthritis trials, allowing quantitative assessment of cartilage thickness and volume, with good accuracy and precision (1, 21). US measurements of cartilage thickness showed high agreement with those with the DESS and reinforced the utility of the DESS as the reference standard. Cartilage thickness excluding the interfacial hypointense layer with FLAIR-FS showed high agreement with that with DESS. In other words, the interfacial hypointense layer with FLAIR-FS should not be included as a part of the cartilage. A composite image of FLAIR-FS and DESS once again confirmed that the hypointense layer was located outside the cartilage. Interestingly, the interfacial hypointense layer continued on the surface of landmark holes where there were full-thickness artificial cartilage defects. These results suggested that the interfacial hypointense layer was located just outside the articular cartilage, and we hypothesized that a restricted water layer was revealed at the cartilage-water interface with FLAIR-FS.

There have been significant difficulties and technical challenges in experimentally testing soft and highly hydrated cartilage in vivo (22). Under natural conditions, when the joint is completely covered with synovial fluid, the surfaces of cartilage appear highly hydrophilic (23). Water molecules may readily adsorb onto hydrophilic surfaces through hydrogen bonding, but it is generally thought that additional ordering is conferred by subsequent hydration layers that build onto the first (24). According to the water structure hypothesis, layers of tightly bound water around the hydrophilic surface and further water layers can build one upon another, beginning at the surface and extending outward. This extensive water structuring results in a hydration layer on the order of 100 μm from the surface (25). Zheng et al. (24) demonstrated unexpectedly thick layers of mobility-limited water in the vicinity of hydrophilic surfaces. In those layers, water diffusion was substantially different from that of bulk water, and water molecules suffered appreciable

restriction. Yoo et al. (26) also demonstrated the existence of highly restricted water layers adsorbed onto hydrophilic surfaces and showed that restricted water has notably shorter T1 relaxation and a smaller self-diffusion coefficient than bulk water. These results suggest that the interfacial hypointense layer we observed is a restricted water layer on the cartilage surface. We now believe that the restricted water layer was nulled at 1500 ms TI, where bulk water was moderately suppressed.

Our study has some limitations. First, we suggest the existence of a restricted water layer on the cartilage surface based on MRI findings, but we have not directly identified this layer. It is necessary to determine whether there are other objective techniques to verify this hypothesis. Second, our experimental cartilage imaging was performed ex vivo in normal saline. Therefore, the results may be different from those in the synovial fluid in vivo. Third, we applied fat suppression in addition to water suppression, as in the previous study (27). Unfortunately, the porcine patella had little bone marrow fat to test the effect of fat suppression. This is the reason why we did not implement fat suppression on T2-weighted imaging. Even so, to assess the clinical use, we needed to study the imaging features of FLAIR combined with fat suppression. Fourth, since we applied a TI of only 1500 ms, we could not compare the effect of different inversion times. Last, we only examined normal cartilage and did not perform histologic examination. For clinical use, studies on FLAIR-FS imaging for damaged cartilage are also needed. We suggest that the above limitations should be supplemented in future research.

In our experiment, FLAIR-FS showed superior contrast between cartilage layers over conventional MR sequences and unveiled a probable restricted water layer immediately next to the cartilage surface. Further basic and clinical research is required to determine the significance of these features of FLAIR-FS in cartilage imaging.

References

1. Crema MD, Roemer FW, Marra MD, Burstein D, Gold GE, Eckstein F, Baum T, Mosher TJ, Carrino JA, Guermazi A. Articular cartilage in the knee: current MR imaging techniques and applications in clinical practice and research. Radiographics 2011;31(1):37-61. doi: 10.1148/rg.311105084

2. Strickland CD, Kijowski R. Morphologic imaging of articular cartilage. Magn Reson Imaging Clin N Am 2011;19(2):229-248. doi: 10.1016/j.mric.2011.02.009

3. Roemer FW, Crema MD, Trattnig S, Guermazi A. Advances in Imaging of Osteoarthritis and Cartilage. Radiology 2011;260(2):332-354. doi: 10.1148/radiol.11101359

4. Recht MP, Resnick D. MR imaging of articular cartilage: current status and future directions. AJR Am J Roentgenol 1994;163(2):283-290. doi: 10.2214/ajr.163.2.8037016

5. Goodwin DW. MRI appearance of normal articular cartilage. Magn Reson Imaging Clin N Am 2011;19(2):215-227. doi: 10.1016/j.mric.2011.02.007

6. Braun HJ, Gold GE. Advanced MRI of articular cartilage. Imaging Med 2011;3(5):541-555. doi: 10.2217/iim.11.43

7. Yoo HJ, Hong SH, Oh HY, Choi JY, Chae HD, Ahn JM, Kang HS. Diagnostic Accuracy of a Fluid-attenuated Inversion-Recovery Sequence with Fat Suppression for Assessment of Peripatellar Synovitis: Preliminary Results and Comparison with Contrast-enhanced MR Imaging. Radiology 2017;283(3):769-778. doi: 10.1148/radiol.2016160155

8. Schwaiger BJ, Gersing AS, Mbapte Wamba J, Nevitt MC, McCulloch CE, Link TM. Can Signal Abnormalities Detected with MR Imaging in Knee Articular Cartilage Be Used to Predict Development of Morphologic Cartilage Defects? 48-Month Data from the Osteoarthritis Initiative. Radiology 2016;281(1):158-167. doi: 10.1148/radiol.2016152308

9. Wendelhag I, Gustavsson T, Suurkula M, Berglund G, Wikstrand J. Ultrasound

measurement of wall thickness in the carotid artery: fundamental principles and description of a computerized analysing system. Clin Physiol 1991;11(6):565-577. doi: 10.1111/j.1475-097x.1991.tb00676.x

10. Steppacher SD, Hanke MS, Zurmuhle CA, Haefeli PC, Klenke FM, Tannast M. Ultrasonic cartilage thickness measurement is accurate, reproducible, and reliable-validation study using contrast-enhanced micro-CT. J Orthop Surg Res 2019;14(1):67. doi: 10.1186/s13018-019-1099-8

11. Faul F, Erdfelder E, Buchner A, Lang A-GJBrm. Statistical power analyses using G* Power 3.1: Tests for correlation and regression analyses. 2009;41(4):1149-1160.

12. Faul F, Erdfelder E, Lang A-G, Buchner AJBrm. G* Power 3: A flexible statistical power analysis program for the social, behavioral, and biomedical sciences. 2007;39(2):175-191.

13. Grunder W. MRI assessment of cartilage ultrastructure. NMR Biomed 2006;19(7):855-876. doi: 10.1002/nbm.1092

14. Recht MP, Goodwin DW, Winalski CS, White LM. MRI of articular cartilage: revisiting current status and future directions. AJR Am J Roentgenol 2005;185(4):899-914. doi: 10.2214/AJR.05.0099

15. Xia Y. Magic-angle effect in magnetic resonance imaging of articular cartilage: a review. Invest Radiol 2000;35(10):602-621. doi: 10.1097/00004424-200010000-00007

16. Paunipagar BK, Rasalkar D. Imaging of articular cartilage. Indian J Radiol Imaging 2014;24(3):237-248. doi: 10.4103/0971-3026.137028

17. Zhang P, Zhao C, Zhao T, Liu M, Jiang L. Recent Advances in Bioinspired Gel Surfaces with Superwettability and Special Adhesion. Adv Sci (Weinh) 2019;6(18):1900996. doi: 10.1002/advs.201900996

18. Choi J-A, Gold GE. MR imaging of articular cartilage physiology. Magnetic resonance imaging clinics of North America 2011;19(2):249-282. doi: 10.1016/j.mric.2011.02.010

19. Jahn S, Seror J, Klein J. Lubrication of Articular Cartilage. Annu Rev Biomed Eng 2016;18:235-258. doi: 10.1146/annurev-bioeng-081514-123305

20. Kumar P, Oka M, Toguchida J, Kobayashi M, Uchida E, Nakamura T, Tanaka K. Role of uppermost superficial surface layer of articular cartilage in the lubrication mechanism of joints. J Anat 2001;199(Pt 3):241-250. doi: 10.1046/j.1469-7580.2001.19930241.x

21. Van Dyck P, Vanhevel F, Vanhoenacker FM, Wouters K, Grodzki DM, Gielen JL, Parizel PM. Morphological MR imaging of the articular cartilage of the knee at 3 T-comparison of standard and novel 3D sequences. Insights Imaging 2015;6(3):285-293. doi: 10.1007/s13244-015-0405-1

22. Graindorge S, Ferrandez W, Jin Z, Ingham E, Grant C, Twigg P, Fisher J. Biphasic surface amorphous layer lubrication of articular cartilage. Med Eng Phys 2005;27(10):836-844. doi: 10.1016/j.medengphy.2005.05.001

23. Pawlak Z, Petelska AD, Urbaniak W, Yusuf KQ, Oloyede A. Relationship between wettability and lubrication characteristics of the surfaces of contacting phospholipid-based membranes. Cell biochemistry and biophysics 2013;65(3):335-345. doi: 10.1007/s12013-012-9437-z

24. Zheng JM, Chin WC, Khijniak E, Khijniak E, Jr., Pollack GH. Surfaces and interfacial water: evidence that hydrophilic surfaces have long-range impact. Advances in colloid and interface science 2006;127(1):19-27. doi: 10.1016/j.cis.2006.07.002

25. Zheng JM, Pollack GH. Long-range forces extending from polymer-gel surfaces. Phys Rev E Stat Nonlin Soft Matter Phys 2003;68(3 Pt 1):031408. doi: 10.1103/PhysRevE.68.031408

26. Yoo H, Paranji R, Pollack GH. Impact of Hydrophilic Surfaces on Interfacial Water Dynamics Probed with NMR Spectroscopy. J Phys Chem Lett 2011;2(6):532-536. doi: 10.1021/jz200057g

27. Yoo HJ, Hong SH, Oh HY, Choi J-Y, Chae HD, Ahn JM, Kang HSJR. Diagnostic accuracy of a fluid-attenuated inversion-recovery sequence with fat suppression for assessment of peripatellar synovitis: preliminary results and comparison with contrast-enhanced MR imaging. 2017;283(3):769-778.

요약 (국문초록)

연구 목적

이 연구는 연골의 지방–물 이중억제 자기공명영상(combined fluid-attenuated inversion recovery with fat suppression, FLAIR-FS)에서 영상 특성을 설명하고, FLAIR-FS의 기본적인 특성과 기존의 자기 공명 영상 기법의 기본적인 특성을 비교해보고자 시행되었다.

연구 방법

14개의 돼지 슬개골을 3 Tesla 자기 공명 영상으로 촬영하였다. 생리식염수가 담긴 용기에 2개의 슬개골을 넣고 고무 밴드로 고정하여 coil에 위치시켰다. MRI 기법으로는 T1 강조영상, T2 강조영상과 반전시간 1500msec을 적용한 FLAIR-FS을 촬영하였다. 14개 연골 중 마지막 2개의 슬개골에 대하여는, 이중에코 항정상태 (double echo steady state, DESS) (TR/TE = 14.5/5.0, flip angle 30°, slice thickness 1.0 mm)와 초음파를 추가로 시행하였다. 14개의 슬개골에 28개의 지점을 표시한 후에, 2명의 근골격계 전문 영상의학과 의사가 5단계의 점수를 활용하여서, T1 강조영상, T2 강조영상과 FLAIR-FS에 대하여 연골 층의 구분 정도를 시각적으로 평가하였다. FLAIR-FS에서 연골-물 계면에서 저신호강도 영역이 예상외로 보였기 때문에, 우리는 이 계면사이의 저신호강도 영역이 연골의 일부인지 아닌지를, FLAIR-FS과 DESS 에서 연골을 비교하여서 평가하였다. DESS와 초음파를 추가로 시행한 2개의 슬개골에서, FLAIR-FS에서 보인 계면 사이의 저신호강도 영역의 위치를 DESS와 상대적으로 평가하기 위하여, FLAIR-FS과 DESS의 혼합 이미지를 만들었다. 또한, FLAIR-FS와 DESS의 연골 두께를 측정하여 비교하였다. FLAIR-FS에 대하여는, 연골 두께를 측정할 때, 두가지의 다른 방법이 사용되었는데, 계면 사이의 저 신호 층을 포함하거나 제외하는 방법으로 측정하였다. DESS에서의 연골 두께 측정의 정확도를 확인하기 위하여, MRI와 초음파에서의 측정이 비교되었다. 측정한

연골두께의 절대 합치도는, 급내상관계수를 이용하여 비교하였고, 95% 신뢰구간을 사용하였다.

연구 결과

FLAIR-FS (반전 시간 1500msec)은 중등도의 물 신호강도 억제를 보였고, 관절연골의 신호강도는 자유로운 물보다 높게 나타났다. 관절 연골은 T1 강조영상, T2 강조영상과 FLAIR-FS 영상 기법에서 세 층 구조를 보였다. 이러한 층 구조는 FLAIR-FS에서 가장 뚜렷하게 구분되어 보였고, 그 다음으로 T2 강조영상, 마지막으로 T1 강조영상 순으로 구분되었다 ($p < 0.001$). FLAIR-FS에서 연골–물 계면에 얇은 저신호강도 영역(두께: 0.7 ± 0.1 mm)이 보였다. 계면 사이의 저신호강도 영역을 제외하였을 때, FLAIR-FS과 DESS의 합성영상에서 연골의 표면이 서로 잘 일치하였다. 연골의 표준 영상인 DESS 기법에서 연골두께는 2.2 ± 0.4mm 였다. DESS와 FLAIR-FS 간 연골두께 측정 결과를 비교하면, 계면 사이의 저신호강도 영역을 제외한 경우(2.3 ± 0.3 mm, 절대합치도 0.904)가, 저신호강도 영역을 포함한 경우 (3.0 ± 0.2 mm, 절대합치도 0.322)보다 더 높은 합치도를 보였다. DESS 기법과 초음파검사의 연골두께 측정의 급내상관계수 절대합치도는 0.919이었다.

결론

지방–물 이중억제 자기공명영상은 연골 층 간의 높은 대조도를 보였고, 연골-물 계면에 움직임이 제한된 물 층의 존재 가능성을 보여주었다.

주요어 : 연골, 자기 공명 영상, 물 억제 영상, 지방 억제
학 번 : 2018-26078